Physics Letters B 706 (2012) 251–255

Contents lists available at SciVerse ScienceDirect

Physics Letters B

www.elsevier.com/locate/physletb

Search for a vector gauge boson in ϕ meson decays with the KLOE detector

KLOE-2 Collaboration

F. Archilli [p,q], D. Babusci [f], D. Badoni [p,q], I. Balwierz [e], G. Bencivenni [f], C. Bini [n,o], C. Bloise [f], V. Bocci [o], F. Bossi [f], P. Branchini [s], A. Budano [r,s], S.A. Bulychjev [i], L. Caldeira Balkeståhl [u], P. Campana [f], G. Capon [f], F. Ceradini [r,s], P. Ciambrone [f], E. Czerwiński [f], E. Dané [f], E. De Lucia [f], G. De Robertis [b], A. De Santis [n,o], G. De Zorzi [n,o], A. Di Domenico [n,o], C. Di Donato [j,k], D. Domenici [f], O. Erriquez [a,b], G. Fanizzi [a,b], G. Felici [f], S. Fiore [n,o], P. Franzini [n,o], P. Gauzzi [n,o], G. Giardina [g,h], S. Giovannella [f,*], F. Gonnella [p,q], E. Graziani [s], F. Happacher [f], B. Höistad [u], L. Iafolla [f], E. Iarocci [l,f], M. Jacewicz [u], T. Johansson [u], A. Kowalewska [v], V. Kulikov [i], A. Kupsc [u], J. Lee-Franzini [f,t], F. Loddo [b], G. Mandaglio [g,h], M. Martemianov [i], M. Martini [f,m], M. Mascolo [p,q], M. Matsyuk [i], R. Messi [p,q], S. Miscetti [f], G. Morello [f], D. Moricciani [q], P. Moskal [e], F. Nguyen [r,s], A. Passeri [s], V. Patera [l,f], I. Prado Longhi [r,s], A. Ranieri [b], C.F. Redmer [u], P. Santangelo [f], I. Sarra [f], M. Schioppa [c,d], B. Sciascia [f], A. Sciubba [l,f], M. Silarski [e], S. Stucci [c,d], C. Taccini [r,s], L. Tortora [s], G. Venanzoni [f], R. Versaci [f,1], W. Wiślicki [v], M. Wolke [u], J. Zdebik [e]

[a] *Dipartimento di Fisica dell'Università di Bari, Bari, Italy*
[b] *INFN Sezione di Bari, Bari, Italy*
[c] *Dipartimento di Fisica dell'Università della Calabria, Cosenza, Italy*
[d] *INFN Gruppo collegato di Cosenza, Cosenza, Italy*
[e] *Institute of Physics, Jagiellonian University, Cracow, Poland*
[f] *Laboratori Nazionali di Frascati dell'INFN, Frascati, Italy*
[g] *Dipartimento di Fisica dell'Università di Messina, Messina, Italy*
[h] *INFN Sezione di Catania, Catania, Italy*
[i] *Institute for Theoretical and Experimental Physics (ITEP), Moscow, Russia*
[j] *Dipartimento di Fisica dell'Università "Federico II", Napoli, Italy*
[k] *INFN Sezione di Napoli, Napoli, Italy*
[l] *Dipartimento di Scienze di Base ed Applicate per l'Ingegneria dell'Università "Sapienza", Roma, Italy*
[m] *Dipartimento di Scienze e Tecnologie applicate, Università "Guglielmo Marconi", Roma, Italy*
[n] *Dipartimento di Fisica dell'Università "Sapienza", Roma, Italy*
[o] *INFN Sezione di Roma, Roma, Italy*
[p] *Dipartimento di Fisica dell'Università "Tor Vergata", Roma, Italy*
[q] *INFN Sezione di Roma "Tor Vergata", Roma, Italy*
[r] *Dipartimento di Fisica dell'Università "Roma Tre", Roma, Italy*
[s] *INFN Sezione di Roma Tre, Roma, Italy*
[t] *Physics Department, State University of New York at Stony Brook, USA*
[u] *Department of Physics and Astronomy, Uppsala University, Uppsala, Sweden*
[v] *National Centre for Nuclear Research, Warsaw, Poland*

ARTICLE INFO

Article history:
Received 3 October 2011
Received in revised form 7 November 2011
Accepted 15 November 2011
Available online 20 November 2011
Editor: M. Doser

Keywords:
e^+e^- collisions
Dark forces
Gauge vector boson

ABSTRACT

The existence of a light dark force mediator has been tested with the KLOE detector at DAΦNE. This particle, called U, is searched for using the decay chain $\phi \to \eta U$, $\eta \to \pi^+\pi^-\pi^0$, $U \to e^+e^-$. No evidence is found in 1.5 fb^{-1} of data. The resulting exclusion plot covers the mass range $5 < M_U < 470$ MeV, setting an upper limit on the ratio between the U boson coupling constant and the fine structure constant, α'/α, of $\leqslant 2 \times 10^{-5}$ at 90% C.L. for $50 < M_U < 420$ MeV.

0370-2693/$ – see front matter
doi:10.1016/j.physletb.2011.11.033

1. Introduction

In recent years, several unexpected astrophysical observations have failed to find a common interpretation in terms of standard astrophysical or particle physics sources. A non-exhaustive list of these observations includes the 511 keV gamma-ray signal from the galactic center observed by the INTEGRAL satellite [1], the excess in the cosmic ray positrons reported by PAMELA [2], the total electron and positron flux measured by ATIC [3], Fermi [4], and HESS [5,6], the annual modulation of the DAMA/LIBRA signal [7,8] and the low energy spectrum of nuclear recoil candidate events observed by CoGeNT [9].

Although there are alternative explanations for some of these anomalies, they could be all explained with the existence of a dark matter weakly interacting massive particle, WIMP, belonging to a secluded gauge sector under which the Standard Model (SM) particles are uncharged [10–19]. An abelian gauge field, the U boson with mass near the GeV scale, couples the secluded sector to the SM through its kinetic mixing with the SM hyper-charge gauge field. The kinetic mixing parameter, ϵ, is expected to be of the order 10^{-4}–10^{-2} [11,20], so that observable effects can be induced in $\mathcal{O}$(GeV)-energy e^+e^- colliders [21,20,22–24] and fixed target experiments [25–28]. The possible existence of a new light boson gauging a new symmetry with a small coupling was in fact already introduced on general grounds in [29], and rediscussed in models postulating also the existence of light spin 0 or 1/2 dark matter particles [30,31]. This boson can have both vector and axial-vector couplings to quark and leptons, however axial couplings are strongly constrained by data, leaving room to vector couplings only.

The U boson can be produced at e^+e^- colliders via different processes: $e^+e^- \to U\gamma$, $e^+e^- \to Uh'$ (h'-strahlung), where h' is a higgs-like particle responsible for the breaking of the hidden symmetry, and $V \to P\gamma$ decays, where V and P are vector and pseudoscalar mesons, respectively. In this work, we study the process $\phi \to \eta U$, using a sample of ϕ mesons produced resonantly at the DAΦNE collider. The U boson can be observed by its decay into a lepton pair, while the η can be tagged by one of its main decays. An irreducible background due to the Dalitz decay of the ϕ meson, $\phi \to \eta\ell^+\ell^-$, is present. This decay has been studied by the SND and CMD-2 experiments, which measured a branching fraction of $\mathrm{BR}(\phi \to \eta e^+e^-) = (1.19 \pm 0.19 \pm 0.07) \times 10^{-4}$ and $\mathrm{BR}(\phi \to \eta e^+e^-) = (1.14 \pm 0.10 \pm 0.06) \times 10^{-4}$, respectively [32,33]. This corresponds to a cross section of $\sigma(\phi \to \eta\ell^+\ell^-) \sim 0.7$ nb, with a di-lepton mass range $M_{\ell\ell} < 470$ MeV. For the signal, the expected cross section is expressed by [22]:

$$\sigma(\phi \to \eta U) = \epsilon^2 \left|F_{\phi\eta}\left(m_U^2\right)\right|^2 \frac{\lambda^{3/2}(m_\phi^2, m_\eta^2, m_U^2)}{\lambda^{3/2}(m_\phi^2, m_\eta^2, 0)} \sigma(\phi \to \eta\gamma), \quad (1)$$

where $F_{\phi\eta}(m_U^2)$ is the $\phi\eta\gamma^*$ transition form factor evaluated at the U mass while the following term represents the ratio of the kinematic functions of the involved decays.[2] Using $\epsilon = 10^{-3}$ and $|F_{\phi\eta}(m_U^2)|^2 = 1$, a cross section $\sigma(\phi \to \eta U) \sim 40$ fb is obtained. Despite the small ratio between the overall cross section of $\phi \to \eta U$ and $\phi \to \eta\ell^+\ell^-$, their different di-lepton invariant mass distributions allow to test the ϵ parameter down to 10^{-3} with the KLOE data set.

The best U decay channel to search for the $\phi \to \eta U$ process at KLOE is in e^+e^-, since a wider range of U boson masses can be tested and $e^\pm$ are easily identified using a time-of-flight (ToF) technique. The η can be tagged by the three-pion or two-photon final state, which represent $\sim 85\%$ of the total decay rate. We have used the $\eta \to \pi^+\pi^-\pi^0$ decay channel, which provides a clean final state with four charged particles and two photons.

2. The KLOE detector

The KLOE experiment operated from 2000 to 2006 at DAΦNE, the Frascati ϕ-factory. DAΦNE is an e^+e^- collider running at a center-of-mass energy of ~ 1020 MeV, the mass of the ϕ meson. Equal energy positron and electron beams collide at an angle of $\pi - 25$ mrad, producing ϕ mesons nearly at rest. The detector consists of a large cylindrical Drift Chamber (DC), surrounded by a lead-scintillating fiber electromagnetic calorimeter (EMC). A superconducting coil around the EMC provides a 0.52 T field. The beam pipe at the interaction region is spherical in shape with 10 cm radius, it is made of a beryllium–aluminum alloy of 0.5 mm thickness. Low beta quadrupoles are located at about ± 50 cm distance from the interaction region. The drift chamber [34], 4 m in diameter and 3.3 m long, has 12,582 all-stereo tungsten sense wires and 37,746 aluminum field wires. The chamber shell is made of carbon fiber-epoxy composite with an internal wall of ~ 1 mm thickness, the gas used is a 90% helium, 10% isobutane mixture. The spatial resolutions are $\sigma_{xy} \sim 150$ μm and $\sigma_z \sim 2$ mm. The momentum resolution is $\sigma(p_\perp)/p_\perp \approx 0.4\%$. Vertexes are reconstructed with a spatial resolution of ~ 3 mm. The calorimeter [35] is divided into a barrel and two endcaps, for a total of 88 modules, and covers 98% of the solid angle. The modules are read out at both ends by photomultipliers, both in amplitude and time. The readout granularity is $\sim (4.4 \times 4.4)$ cm^2, for a total of 2440 cells arranged in five layers. The energy deposits are obtained from the signal amplitude while the arrival times and the particles positions are obtained from the time differences. Cells close in time and space are grouped into energy clusters. The cluster energy E is the sum of the cell energies. The cluster time T and position $\vec{R}$ are energy-weighted averages. Energy and time resolutions are $\sigma_E/E = 5.7\%/\sqrt{E\ (\mathrm{GeV})}$ and $\sigma_t = 57\ \mathrm{ps}/\sqrt{E\ (\mathrm{GeV})} \oplus 100$ ps, respectively. The trigger [36] uses both calorimeter and chamber information. In this analysis the events are selected by the calorimeter trigger, requiring two energy deposits with $E > 50$ MeV for the barrel and $E > 150$ MeV for the endcaps. A cosmic veto rejects events with at least two energy deposits above 30 MeV in the outermost calorimeter layer. Data are then analyzed by an event classification filter [37], which selects and streams various categories of events in different output files.

3. Event selection

The analysis of the decay chain $\phi \to \eta U$, $\eta \to \pi^+\pi^-\pi^0$, $U \to e^+e^-$, has been performed on a data sample of 1.5 fb^{-1}, corresponding approximately to 5×10^9 produced ϕ mesons. The Monte Carlo (MC) simulation of the irreducible background $\phi \to \eta e^+e^-$, $\eta \to \pi^+\pi^-\pi^0$ has been produced with $d\Gamma(\phi \to \eta e^+e^-)/dm_{ee}$ weighted according to Vector Meson Dominance model [38], using the form factor parametrization from the SND experiment [32]. The MC simulation for the $\phi \to \eta U$ decay has been developed according to [22], with a flat distribution in M_{ee}. All MC productions, including all other ϕ decays, take into account changes in DAΦNE operation and background conditions on a run-by-run basis. Data-MC corrections for cluster energies and tracking efficiency, evaluated with radiative Bhabha events and $\phi \to \rho\pi$ samples, respectively, have been applied.

As a first step of the analysis, a preselection is performed requiring:

* Corresponding author.
E-mail address: simona.giovannella@lnf.infn.it (S. Giovannella).
[1] Present address: CERN, CH-1211 Geneva 23, Switzerland.
[2] $\lambda(m_1^2, m_2^2, m_3^2) = [1 + m_3^2/(m_1^2 - m_2^2)]^2 - 4m_1^2m_3^2/(m_1^2 - m_2^2)^2$.

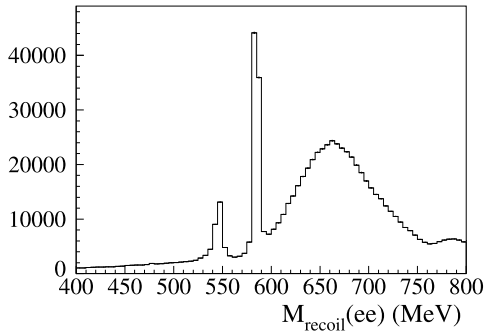

Fig. 1. Recoiling mass against the e^+e^- pair for the data sample after preselection cuts. The $\phi \to \eta e^+e^-$ signal is clearly visible in the peak corresponding to η mass. The second peak at ~ 590 MeV is due to $\phi \to K_S K_L$, $K_S \to \pi^+\pi^-$ events with wrong mass assignment.

(1) two positive and two negative tracks with point of closest approach to the beam line inside a cylinder around the interaction point (IP), with transverse radius $R_{\rm FV} = 4$ cm and length $Z_{\rm FV} = 20$ cm;
(2) two photon candidates *i.e.* two energy clusters with $E > 7$ MeV not associated to any track, in an angular acceptance $|\cos\theta_\gamma| < 0.92$ and in the expected time window for a photon ($|T_\gamma - R_\gamma/c| < \min(5\sigma_T, 2$ ns));
(3) best $\pi^+\pi^-\gamma\gamma$ match to the η mass in the pion hypothesis to assign $\pi^\pm$ tracks[3]; the other two tracks are then assigned to $e^\pm$;
(4) loose cuts of about $\pm 4\sigma$'s on η and π^0 invariant masses ($495 < M_{\pi^+\pi^-\gamma\gamma} < 600$ MeV, $70 < M_{\gamma\gamma} < 200$ MeV).

After this selection, a clear peak corresponding to $\phi \to \eta e^+e^-$ events is observed in the distribution of the recoil mass to the e^+e^- pair, $M_{\rm recoil}(ee)$, as shown in Fig. 1. The second peak at ~ 590 MeV is due to $K_S \to \pi^+\pi^-$ events with a wrong mass assignment. Events in the $535 < M_{\rm recoil}(ee) < 560$ MeV window are retained for further analysis.

A residual background contamination, due to $\phi \to \eta\gamma$ events with photon conversion on beam pipe (BP) or drift chamber walls (DCW), is rejected by tracing back the tracks of the two e^+, e^- candidates and reconstructing their invariant mass (M_{ee}) and distance (D_{ee}) at the BP/DCW surfaces. As both quantities are small in case of photon conversions, $\phi \to \eta\gamma$ background is removed by rejecting events with: $M_{ee}({\rm BP}) < 10$ MeV and $D_{ee}({\rm BP}) < 2$ cm, $M_{ee}({\rm DCW}) < 80$ MeV and $D_{ee}({\rm DCW}) < 10$ cm. A further relevant background, originated by $\phi \to K\bar{K}$ decays surviving analysis cuts, has more than two charged pions in the final state and is suppressed using time-of-flight (ToF) to the calorimeter. When an energy cluster is connected to a track, the arrival time to the calorimeter is evaluated both using the calorimeter timing ($T_{\rm cluster}$) and the track trajectory ($T_{\rm track} = L_{\rm track}/\beta c$). The $\Delta T = T_{\rm track} - T_{\rm cluster}$ variable is then evaluated in both electron (ΔT_e) and pion (ΔT_π) hypotheses. Events with an e^+, e^- candidate outside a 3σ window on the ΔT_e variables are rejected. In Fig. 2, the M_{ee} distribution evaluated at different steps of the analysis is shown. The peaks at ~ 30 MeV and ~ 80 MeV are due to photon conversions on BP and DCW, respectively. The ToF cut reduces the tail at high M_{ee} values while the conversion cut removes events in the low invariant mass region. The analysis efficiency, defined as the ratio between the number of events surviving analysis cuts and that of all generated events, is shown in Fig. 3 as a function of M_{ee}, ranging between 10% and 20%. The main contribution to the loss of efficiency is due to preselection cuts, being $\varepsilon_{\rm presel} = (24.73 \pm 0.04)\%$.

[3] The invariant mass of $\pi^+\pi^-\gamma\gamma$ for each positive/negative track pair, $M_{\rm test}$, is evaluated in the hypothesis that the two tracks belong to charged pions. The track pair with the smaller $|M_{\rm test} - M_\eta|$ value is assigned to π^+ and π^-.

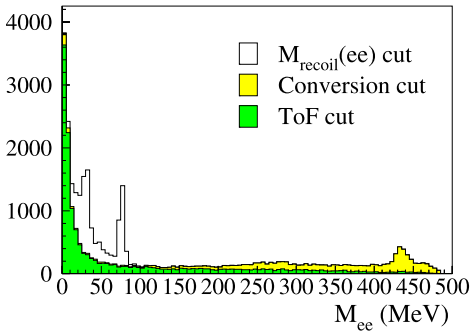

Fig. 2. M_{ee} distribution for data after different analysis cuts.

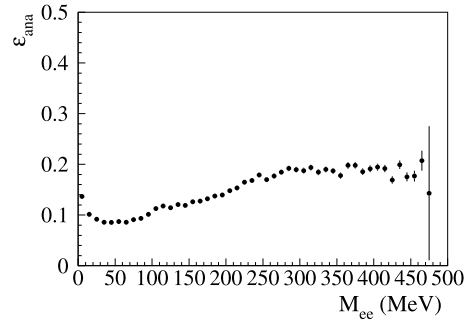

Fig. 3. Analysis efficiency as a function of e^+e^- invariant mass.

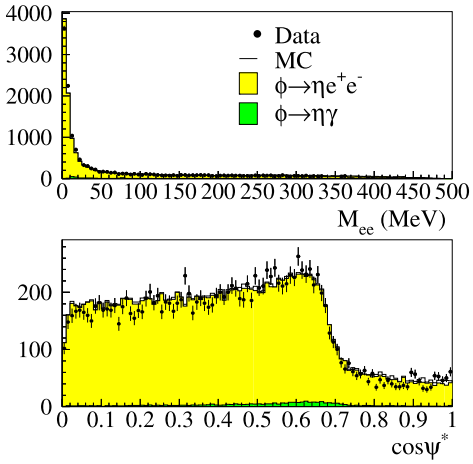

Fig. 4. Invariant mass of the e^+e^- pair (top) and $\cos\psi^*$ distribution (bottom) for $\phi \to \eta e^+e^-$, $\eta \to \pi^+\pi^-\pi^0$ events. Dots are data, the black solid line is the sum of all MC expectations while signal and residual background contamination from $\phi \to \eta\gamma$ are shown in colors.

In Fig. 4 the comparison between data and Monte Carlo events for M_{ee} and $\cos\psi^*$ distributions is shown. Here ψ^* is the angle between the η and the e^+ in the e^+e^- rest frame. About 14,000 $\phi \to \eta e^+e^-$, $\eta \to \pi^+\pi^-\pi^0$ candidates are present in the analyzed data set, with a negligible residual background contamination.

4. Upper limit evaluation

As an accurate description of the background is crucial for the search of the U boson, its shape is extracted directly from our data. A fit is performed to the M_{ee} distribution, after applying a bin-by-bin subtraction of the $\phi \to \eta\gamma$ background and efficiency

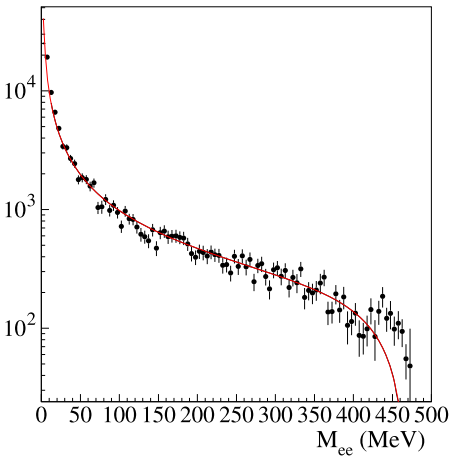

Fig. 5. Fit to the corrected M_{ee} spectrum for the Dalitz decays $\phi \to \eta e^+ e^-$.

correction. The parametrization of the fitting function has been taken from Ref. [38]:

$$\frac{d\Gamma(\phi \to \eta e^+ e^-)}{dq^2} = \frac{\alpha}{3\pi}\frac{|F_{\phi\eta}(q^2)|^2}{q^2}\sqrt{1-\frac{4m^2}{q^2}}\left(1+\frac{2m^2}{q^2}\right)\lambda^{3/2}(m_\phi^2, m_\eta^2, m_U^2) \quad (2)$$

with $q = M_{ee}$ and the transition form factor described by

$$F_{\phi\eta}(q^2) = \frac{1}{1 - q^2/\Lambda^2}. \quad (3)$$

Free parameters of the fit are Λ and an overall normalization factor. A good description of the M_{ee} shape is obtained except at the high end of the spectrum (see Fig. 5), where a residual background contamination from multi-pion events is still present.

As mentioned in Section 3, the $\phi \to \eta U$ MC signal has been produced according to Ref. [22], with a flat distribution of the U boson invariant mass, M_U. This sample has been used to evaluate the resolution on the e^+e^- invariant mass as a function of M_U, applying a Gaussian fit to the $M_{ee} - M_U$ distributions. Results are reported in Fig. 6. The resolution is ~ 2 MeV for $M_U < 350$ MeV and then improves to 1 MeV for higher values. The upper limit on $\phi \to \eta U$ signal as a function of M_U is then obtained in the following way:

(a) MC events are divided in sub-samples of 1 MeV width in the range $5 < M_U < 470$ MeV;
(b) for each M_U sub-sample, the average value of the $\phi \to \eta e^+ e^-$ background, $b(M_{ee})$, is obtained by fitting the reconstructed M_{ee} spectrum with 5 MeV binning, removing five bins centered at M_U;
(c) for each fit, the maximum variation of $b(M_{ee})$ events, $\Delta b(M_{ee})$, is obtained changing by $\pm 1\sigma$ the fit parameters;
(d) for each M_U value, the signal hypothesis is tested comparing observed data, $b(M_{ee})$ and MC signal in the five reconstructed bins excluded in (b). The exclusion plot is obtained applying the CLs method [39]. A Gaussian spread of width $\Delta b(M_{ee})$ on the background distribution is applied while evaluating CLs.

In Fig. 7 the exclusion plot at 90% C.L. on the number of events for the decay chain $\phi \to \eta U$, $\eta \to \pi^+\pi^-\pi^0$, $U \to e^+e^-$, is shown. Using Eq. (1) and taking into account the analysis efficiency this result is then reported in terms of the parameter $\alpha'/\alpha = \epsilon^2$, where α' is the coupling of the U boson to electrons and α is the fine

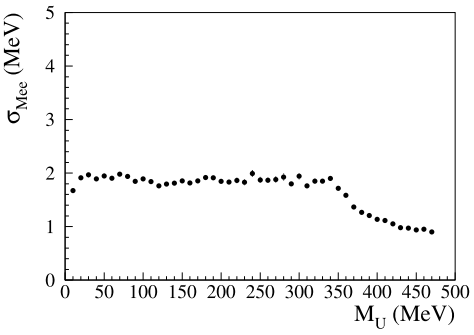

Fig. 6. Resolution on M_{ee} as a function of the U boson invariant mass for $\phi \to \eta U$ MC events.

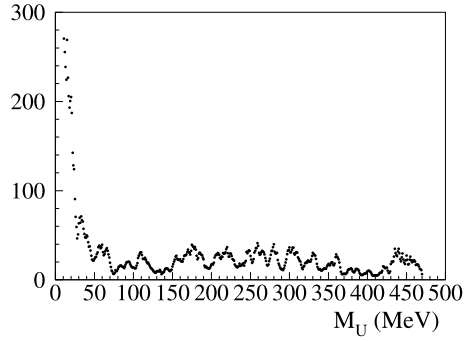

Fig. 7. Upper limit at 90% C.L. on the number of events for the decay chain $\phi \to \eta U$, $\eta \to \pi^+\pi^-\pi^0$, $U \to e^+e^-$.

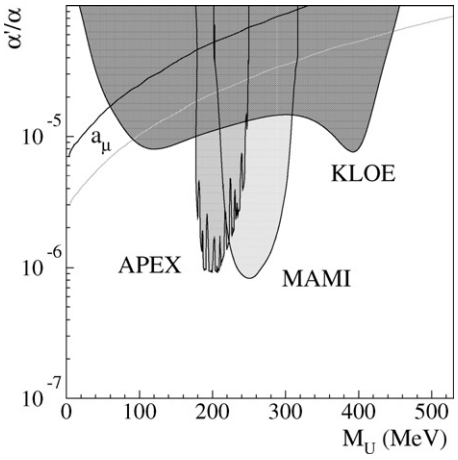

Fig. 8. Exclusion plot at 90% C.L. for the parameter $\alpha'/\alpha = \epsilon^2$, compared with existing limits in our region of interest.

structure constant. The opening of the $U \to \mu^+\mu^-$ threshold, in the hypothesis that the U boson decays only to lepton pairs and assuming equal coupling to e^+e^- and $\mu^+\mu^-$, has been included. In Fig. 8 the smoothed exclusion plot at 90% C.L. on α'/α is compared with existing limits from the muon anomalous magnetic moment a_μ [40] and from recent measurements of the MAMI/A1 [41] and APEX [42] experiments. The gray line is where the U boson parameters should lay to account for the observed discrepancy between measured and calculated a_μ values. Our result greatly improves existing limits in a wide mass range, resulting in an upper limit on the α'/α parameter of $\leqslant 2 \times 10^{-5}$ @ 90% C.L. for $50 < M_U < 420$ MeV, thus covering part of the expected ϵ range (see Section 1). We exclude that the existing a_μ discrepancy is due to a U boson with mass ranging between 90 and 450 MeV.

Acknowledgements

We warmly thank our former KLOE colleagues for the access to the data collected during the KLOE data taking campaign. We thank the DAΦNE team for their efforts in maintaining low background running conditions and their collaboration during all data taking. We want to thank our technical staff: G.F. Fortugno and F. Sborzacchi for their dedication in ensuring efficient operation of the KLOE computing facilities; M. Anelli for his continuous attention to the gas system and detector safety; A. Balla, M. Gatta, G. Corradi and G. Papalino for electronics maintenance; M. Santoni, G. Paoluzzi and R. Rosellini for general detector support; C. Piscitelli for his help during major maintenance periods. This work was supported in part by the EU Integrated Infrastructure Initiative HadronPhysics Project under contract number RII3-CT-2004-506078; by the European Commission under the 7th Framework Programme through the 'Research Infrastructures' action of the 'Capacities' Programme, Call: FP7-INFRASTRUCTURES-2008-1, Grant Agreement No. 227431; by the Polish Ministery of Science and Higher Education through the Grant No. 0469/B/H03/2009/37.

References

[1] P. Jean, et al., Astron. Astrophys. 407 (2003) L55.
[2] O. Adriani, et al., Nature 458 (2009) 607.
[3] J. Chang, et al., Nature 456 (2008) 362.
[4] A.A. Abdo, et al., Phys. Rev. Lett. 102 (2009) 181101.
[5] F. Aharonian, et al., Phys. Rev. Lett. 101 (2008) 261104.
[6] F. Aharonian, et al., Astron. Astrophys. 508 (2009) 561.
[7] R. Bernabei, et al., Int. J. Mod. Phys. D 13 (2004) 2127.
[8] R. Bernabei, et al., Eur. Phys. J. C 56 (2008) 333.
[9] C.E. Aalseth, et al., Phys. Rev. Lett. 107 (2011) 141301.
[10] M. Pospelov, A. Ritz, M.B. Voloshin, Phys. Lett. B 662 (2008) 53.
[11] N. Arkani-Hamed, D.P. Finkbeiner, T.R. Slatyer, N. Weiner, Phys. Rev. D 79 (2009) 015014.
[12] D.S.M. Alves, S.R. Behbahani, P. Schuster, J.G. Wacker, Phys. Lett. B 692 (2010) 323.
[13] M. Pospelov, A. Ritz, Phys. Lett. B 671 (2009) 391.
[14] J. Hisano, S. Matsumoto, M.M. Nojiri, Phys. Rev. Lett. 92 (2004) 031303.
[15] M. Cirelli, M. Kadastik, M. Raidal, A. Strumia, Nucl. Phys. B 813 (2009) 1.
[16] J. March-Russell, S.M. West, D. Cumberbatch, D. Hooper, JHEP 0807 (2008) 058.
[17] I. Cholis, G. Dobler, D.P. Finkbeiner, L. Goodenough, N. Weiner, Phys. Rev. D 80 (2009) 123518.
[18] I. Cholis, D.P. Finkbeiner, L. Goodenough, N. Weiner, JCAP 0912 (2009) 007.
[19] N. Arkani-Hamed, N. Weiner, JHEP 0812 (2008) 104.
[20] R. Essig, P. Schuster, N. Toro, Phys. Rev. D 80 (2009) 015003.
[21] B. Batell, M. Pospelov, A. Ritz, Phys. Rev. D 79 (2009) 115008.
[22] M. Reece, L.T. Wang, JHEP 0907 (2009) 051.
[23] N. Borodatchenkova, D. Choudhury, M. Drees, Phys. Rev. Lett. 96 (2006) 141802.
[24] P.F. Yin, J. Liu, S.h. Zhu, Phys. Lett. B 679 (2009) 362.
[25] J.D. Bjorken, R. Essig, P. Schuster, N. Toro, Phys. Rev. D 80 (2009) 075018.
[26] B. Batell, M. Pospelov, A. Ritz, Phys. Rev. D 80 (2009) 095024.
[27] R. Essig, P. Schuster, N. Toro, B. Wojtsekhowski, JHEP 1102 (2011) 009.
[28] M. Freytsis, G. Ovanesyan, J. Thaler, JHEP 1001 (2010) 111.
[29] P. Fayet, Phys. Lett. B 95 (1980) 285;
P. Fayet, Phys. Lett. B 187 (1981) 184.
[30] C. Boehm, P. Fayet, Nucl. Phys. B 683 (2004) 219.
[31] P. Fayet, Phys. Rev. D 70 (2004) 023514.
[32] M.N. Achasov, et al., Phys. Lett. B 504 (2001) 275.
[33] R.R. Akhmetshin, et al., Phys. Lett. B 501 (2001) 191.
[34] M. Adinolfi, et al., Nucl. Instr. Meth. A 488 (2002) 51.
[35] M. Adinolfi, et al., Nucl. Instr. Meth. A 482 (2002) 364.
[36] M. Adinolfi, et al., Nucl. Instr. Meth. A 492 (2002) 134.
[37] F. Ambrosino, et al., Nucl. Instr. Meth. A 534 (2004) 403.
[38] L.G. Landsberg, Phys. Rep. 128 (1985) 301.
[39] T. Junk, Nucl. Instr. Meth. A 434 (1999) 435.
[40] M. Pospelov, Phys. Rev. D 80 (2009) 095002.
[41] H. Merkel, et al., Phys. Rev. Lett. 106 (2011) 251802.
[42] S. Abrahamyan, et al., Phys. Rev. Lett. 107 (2011) 191804.